

Terahertz Circular Dichroism Spectroscopy of Biomolecules.

Jing Xu^a, Jhenny Galan^b, Gerry Ramian^c, Pavlos Savvidis^c,
Anthony Scopatz^a, Robert R. Birge^b, S. James Allen^{a,c,d}, Kevin Plaxco^{d,e}

^aPhysics Department, UCSB, Santa Barbara, CA 93106;

^bBiological and Physical Chemistry, University of Connecticut, Storrs, CT 06269

^cInstitute for Quantum Engineering, Science and Technology, UCSB, Santa Barbara, CA 93106

^dCenter for Polymer and Organic Solids, UCSB, Santa Barbara, CA 93106

^eDepartment of Chemistry and Biochemistry, UCSB, Santa Barbara, CA 93106

ABSTRACT

Biopolymers such as proteins, DNA and RNA fold into large, macromolecular chiral structures. As charged macromolecules, they absorb strongly in the terahertz due to large-scale collective vibrational modes; as chiral objects, this absorption should be coupled with significant circular dichroism. Terahertz circular dichroism (TCD) is potentially important as a biospecific sensor, unobscured by spectral features related to abiological material. We have constructed atomistic simulations and elastic continuum models of TCD. These models estimate the magnitude of the TCD and the relation between TCD spectroscopic signatures (zero crossings) and the structure, charge distribution and mechanical properties of biomaterials. A broad band TCD spectrometer based on a polarizing interferometer is developed to explore TCD in biomolecules in aqueous solution. Preliminary results on TCD in lysozyme in water at several terahertz frequencies is presented.

Keywords: proteins, collective vibrational modes, sub-millimeter, Far-IR, terahertz, circular dichroism, chiral molecule

1. INTRODUCTION

Biopolymers are not the static conformations so beautifully illustrated in crystallographic structures that appear in textbooks. Proteins and nucleic acids are, instead, dynamic across a wide range of length- and time-scales with molecular motions thought to play a fundamental, if poorly understood, role in all of their physical and, in many cases, functional properties.

The ability of biomolecules to deform is critical to their participation in biological activity. For example, it has been recognized for forty years that the binding of O₂ to myoglobin requires rapid, large scale “breathing” motions of the protein in order for the ligand to access the heme iron¹. Countless other examples include the collective motions in transmembrane receptors and bacteriorhodopsin (bR), which undergo enormous conformational changes upon ligand binding or ligand isomerization and thereby regulate or drive cellular processes². Incontrovertible experimental evidence demonstrates that many examples of structural plasticity are under intense selective pressure: mutations that alter the conformational rigidity of proteins and nucleic acids can lead to complete loss of function³.

Theoretical studies paint a picture consistent with the importance of dynamics in biopolymer structure and function and suggest that proteins and nucleic acids are well-populated with global and sub-global dynamic modes in the THz regime⁴. For

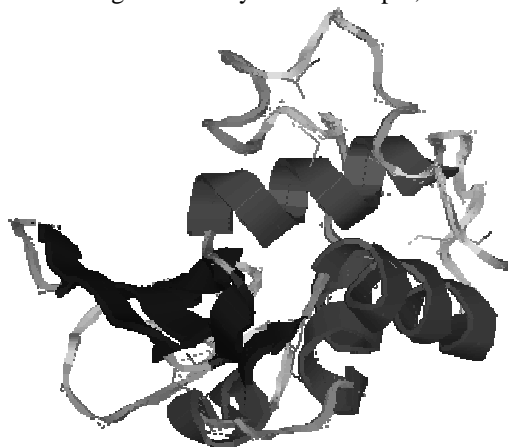


Fig. 1 Inter-domain collective modes in biopolymers, such as the protein lysozyme occur at THz frequencies.

example, normal mode calculations indicate that the two domains of the protein lysozyme (Fig. 1) behave approximately as a harmonic oscillator with many collective modes in the frequency range 0.03 – 15 THz⁵. Prohofsky and co-workers have analyzed short chain DNA molecules and identified twisting and librational modes in the range 0.6 – 3 THz⁶. Similarly, protein collective vibrational modes have been calculated to lie in this spectral region for bovine pancreatic trypsin inhibitor⁷, hen egg white lysozyme⁸ and myoglobin⁹. All of these modes arise due to collective, relative motions between tertiary subunits in the biopolymer or coherent movements within a subunit. THz dynamic modes represent the functionally relevant, global motions of biopolymers.

Circular dichroism (CD), the different absorption for right versus left circularly polarized radiation can only occur in the presence of chiral media. Given that all macromolecules with ionic or polar constituents absorb strongly across the terahertz part of the spectrum^{10,11,12} and that biomaterials are enantiomerically pure (i.e., net chiral), biomaterials should be a strong source of CD in the THz. This CD will be related to the macromolecular organization and macromolecular low frequency terahertz vibrations of the biomolecules. Since the abiological materials are not chiral, (TCD) can provide a spectroscopy or “fingerprinting” sensitive to the macromolecular structure but unobscured by spectral features associated with the abiological material. As we discuss below the TCD spectral signature should be a series of “zero crossings” that could be “read” like a bar code; spectral signatures are not resonant peaks and positions but rather zero crossings.

In the following we develop some simple models to guide the development of this new terahertz spectroscopy, describe a TCD spectrometer, show preliminary results on TCD in lysozyme and then indicate future direction.

2. MODELS OF TERAHERTZ CIRCULAR DICHROISM.

While *ab initio* methods have been used to successfully calculate the CD spectra of small molecules, the direct calculation of CD features arising from the collective vibrational modes of macromolecules are computationally intractable. In an effort to develop our intuition about the possible magnitude of the TCD effect we resort to calculating the TCD spectra generated by two simple physical models of the relevant molecular motions.

Models of vibrational CD have been explored but these have largely focused on spectra in the near-infrared, spectra dominated by bond stretching and bending, and the wagging of small subunits in a macromolecule^{13,14,15,16}. The terahertz part of the spectrum couples to vibrations of the entire macromolecule, or large subunits thereof, and requires a model that explores large scale, collective vibrations. In collective vibrations nearest neighbor atoms move together, with large relative motions being experienced only by pairs of atoms that are widely separated in the macromolecule. An important consideration is that, as these low frequency macromolecular vibrations soften, they resolve into large amplitude conformational changes that are widely held to be biologically (functionally) relevant¹⁷.

2.1 Mass and spring model.

Given the prevalence of helical sub-structures in biopolymers such as proteins, DNA and RNA, we are compelled to explore a “mass and spring” model of a helical molecular structure as a simple physical representation that captures the essential features of biological macromolecules. Here we eschew as much detail as possible and strive for the simplest model that produces TCD and that we can manipulate to develop some intuition about spectral signatures and their order of magnitude.

Our model is comprised of a simple collection of masses distributed uniformly in a helical pattern (Fig. 2). Each mass represents more than a simple atom or ion; it represents the covalently bonded atom on the backbone and whatever is attached to it. We assume that these units interact only with their nearest neighbors. For

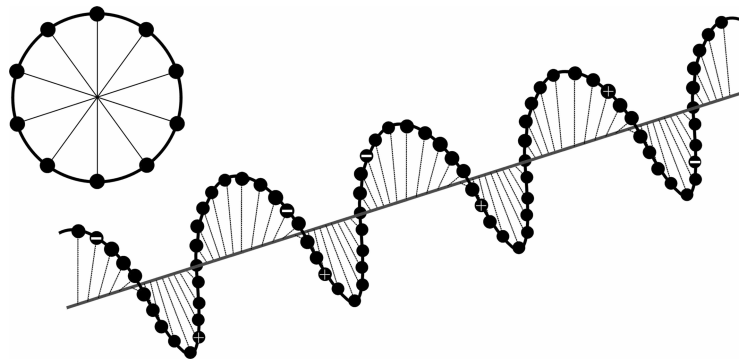


Fig. 2 Mass and spring model distributes masses uniformly but distributes charge non-uniformly to couple various acoustic modes to the electromagnetic field. Upper left is an axial view of the helix.

the sake of simplicity we assume all masses are the same and we treat only the torsional motion of the masses about the axis of the helix. This model will produce acoustic-like torsional modes. For simplicity we do not consider radial and longitudinal acoustic modes. To couple to the propagating terahertz electromagnetic field and produce a polarization that attenuates and alters the speed of the electromagnetic wave, charge must be distributed along the helix. The parameters used, which roughly approximate the α -helix of proteins, are the following: period of the helix, 0.55 nm; masses/period, 10; charge distribution, $-5e/14$ sites; highest frequency acoustic mode, 10 THz; volume density or helix period/ m^3 , $0.9 \times 10^{27} m^{-3}$, relaxation time, $0.53 \times 10^{-12} s$.

The torsional acoustic modes supported by our specific model of the helix are shown (Fig. 3). As in linear chain models of acoustic modes in solids, the highest frequency mode corresponds to an acoustic wavelength of $\lambda_{\max} = 2a$, twice the site spacing. This particular calculation assumes that the helix is infinitely long. A finite helix will support additional standing waves with wavelengths determined by the boundary conditions at the ends. If, guided by typical examples (*e.g.* Fig. 1), we take the helix to be 7 periods long we estimate that the longest wavelength is approximately $\lambda_{\max} = 140a$, corresponding to a frequency of ~ 0.5 THz.

In reality, the excitation of the helix in the biomolecule is not uniform; there are a variety of masses, extraneous coupling to the environment, different charges and different local field corrections. The electromagnetic field, very nearly uniform on the length scale of the helix, drive a variety of modes determined by the Fourier transform of the charge coupling parameters along the helix. Here we have simply placed a charge every 14 sites to simulate a very nonuniform excitation of the helix. The consequences of this particular distribution of charge are shown (Fig. 3). The electromagnetic field at a given frequency will resonate with a torsional acoustic mode at a wavevector determined by the dispersion relation, but produces amplitude exhibiting resonant behavior at acoustic wavelengths or wavevectors determined by the spatial variation of the charge in the helix. We can conclude that a particular helix will have a signature determined by among other things the distributions of mass and charge.

We have calculated the polarization produced by a linearly polarized electromagnetic wave and find that in addition to the polarization in the direction of the applied terahertz electric field, the system produces polarization perpendicular to it and with the symmetry properties¹⁸ required to produce rotation or TCD. Several relevant features are observed in the resulting resonant absorption and resonant TCD. As expected, the helical model absorbs strongly at the frequencies corresponding to the resonant excitation shown (Fig. 3, middle). For the model density, the absorption is quite strong. Indeed, it is well known that all glasses with reasonable charge density, such as the glass from sodium silicate, exhibit strong terahertz absorption that strengthens with increasing frequency. The TCD spectral features consist of a series of zero crossings (Fig. 3, bottom). In the simple model the resonant features are simply determined by the distribution of charges. We may expect that any particular helical unit exhibits a unique, broad band “signature” or pattern of such zero crossings.

CD is always a small fraction of the direct absorption. Using visible, UV or infrared ratios as a guide we would expect that the ratio will be $\sim a/\lambda_{THz}$, where a is of the order of the atom or ion spacing. This is a very small number at terahertz frequencies. But the molecular unit, “terahertz chromophore” that is responsible for the terahertz absorption involves

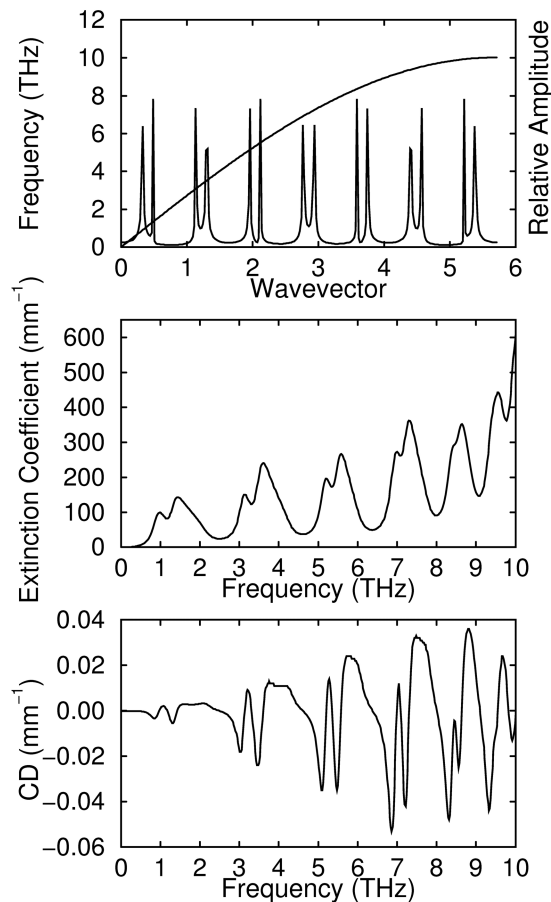


Fig. 3 Top: The dispersion relation for acoustic torsional modes on the model helix. The relative amplitude of a mode excited at a given THz frequency or wavevector. Middle: Extinction coefficient versus frequency. Bottom: THz CD versus frequency.

many atoms and ions¹⁵. For a helix 7 periods in length, the long wavelength acoustic mode in our simple model is $\sim 140a$ and we expect to recover CD to absorption ratios that are reasonable relative to those of electronic excitations or near infrared vibrations. For this particular, rather simple model we find $\Delta\epsilon/\epsilon \sim 10^{-4}$, suggesting that TCD may be at least as intense as CD at optical wavelengths. We thus conclude that the macromolecular vibrations of the helical structures inside typical biomolecules are likely to lead to reasonably strong but complex TCD spectra.

2.2 Normal mode analysis.

While simple, generic models can provide important insights into the general issue of macromolecular TCD, it is also important to explore whether similar effects are present in more realistic models of biopolymers. To this end we have also performed detailed calculations of the TCD spectra of a specific, representative biopolymer, the archeal protein bacteriorhodopsin (Fig. 4). Normal mode calculations¹⁹ were performed to analyze the low-frequency modes in the native protein (wild type, WT) and a version of the protein

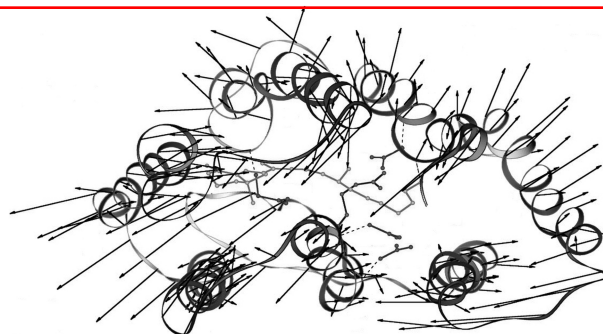


Fig. 4 Schematic diagram of the protein bacteriorhodopsin. Only the backbone of the polymer and a few key side chains are illustrated. Indicated by arrows are the atomic motions involved in the protein's low frequency mode at 0.498 THz. The length of the arrows is proportional to the motion of the element involved, but is exaggerated to facilitate viewing.

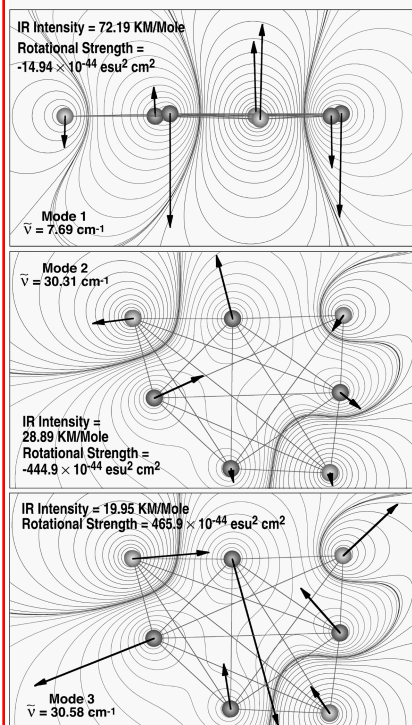
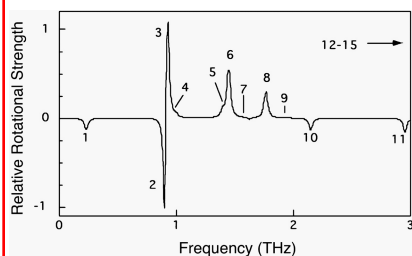


Fig. 5 Simplified normal mode analysis and resulting terahertz circular dichroism (top).

containing a single mutation in which the residue aspartate-96 is replaced with asparagine (D96N).

There are a total of 268 calculated modes below 3 THz, approximately 20% of which are strongly allowed. The most intense modes involve concerted motions of entire helices, a representative example of which is illustrated (Fig. 4). We simulate the TCD activity of these modes using charged heavy masses to simulate entire helices connected by harmonic springs (Fig. 5). Only some of the resultant modes are reflective of the modes observed in a protein. The lowest frequency mode (mode 1) is an out-of-plane distortion that has no direct analogy in the bands calculated for bacteriorhodopsin. In contrast, modes 2 and 3 of our simulation have much in common with the in plane helix translocation modes that characterize the terahertz vibrations in bacteriorhodopsin. The fact that such modes consistently yield intense TCD bands is logical because the charged unit is vibrating within a chiral arrangement. Based on these simulations we propose that a majority of the strong protein vibrational modes below 3 THz will have observable TCD activity with rotatory strengths in the range $10^{-42} - 10^{-41} \text{ esu}^2 \text{ cm}^2$ ($10^{-65} - 10^{-64} \text{ C}^2 \text{ m}^2$). However, the fact that individual modes have TCD activity does not guarantee that the net TCD spectrum of the biomolecule will be intense. This observation follows from the fact that two nearby modes can have similar but opposite rotational strengths (e.g. modes 2 and 3 in Fig. 5). As the density of vibrational modes increases, the probability of accidental cancellations of net rotational strength will increase. Our simulations indicate that the density of modes increases as the vibrational energy increase, and it is possible that large proteins may yield such a high density of TCD modes above 2 THz that the average rotational strength will start to decrease at energies near or above this frequency. A definitive answer to this hypothesis is beyond the capability of our current models and thus provides further impetus for experimental studies of TCD.

We have also investigated the contributions of hydration shells to likely biomolecular TCD signatures. Although water is the principal constituent of biological systems, it is achiral, and thus bulk water will not exhibit TCD. Approximately 1-5% of the water in a cell, however, is "biological water" that is in direct association with polar or charged groups on the surface or inside of

proteins and nucleic acids and may, due to this “induced chirality,” be CD-active. In order to test this, we have carried out a series of calculations on biological water using Hartree-Fock and density functional (B3LYP) methods. An important outcome of these studies is the observation that, by weight, biological water will likely be the single most important source of a TCD signature of a hydrated biological system. We find two sources of contribution. The first is solvation enhancement. When water is added to a system, it stabilizes ionic species through direct association with the polar and charged amino acids. When these residues participate in low frequency, large amplitude vibrational motion, the hydration shell moves to maintain stabilization of the polar or charged species. The net result is a lowering of the frequency and an enhancement in the intensity of the signal. The frequency is lowered because the mass of the vibrating system has increased. The intensity increases because the magnitude of the charges is enhanced through solvation. Because a chiral sub-system imparts chirality on the super-system, the first hydration shell enhances the chirality of the local protein environment. The second hydration shell tends to slightly diminish the chirality due to fluid motion, and subsequent shells have relatively little impact. In all cases we investigated, however, water enhanced the TCD signature. We have also observed specific cases of very intense TCD signals associated with water “wires” that bridged the gap between two charged residues. In the five examples studied, water wires containing from three to seven molecules exhibited low frequency modes in the 0.3 - 3 THz region, and many of these modes had rotatory strengths above 10^{-42} esu² cm². From a mass-weighted perspective, water wires between charged residues were the single most important source of TCD bands that we observed in our simulations.

2. TERAHERTZ CIRCULAR DICHROISM SPECTROMETER

A schematic diagram of the TCD spectrometer is shown in Fig. 6. The radiation is delivered from the UCSB free-electron lasers that can be tuned from 120 GHz to 4.8 THz. Although they deliver high peak power, they have a low duty cycle. (Peak powers are kilowatts; average powers are milliwatts.) This has important implications if we project to a future TCD biosensor. Average power is important here and tunable terahertz harmonic generators can generate average powers of 10’s of milliwatts. The UCSB free-electron lasers are a very convenient research tool as we explore for the first time TCD, but if this approach to bio-sensing is viable they can be replaced by solid-state sources like those

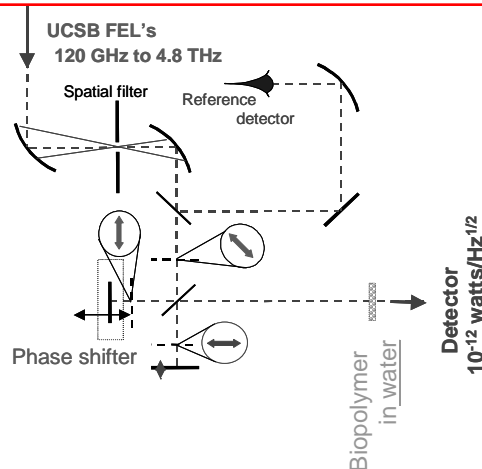


Fig. 6 Schematic diagram of the TCD spectrometer driven by the UCSB free-electron lasers.

developed by Crowe and co-workers²⁰.

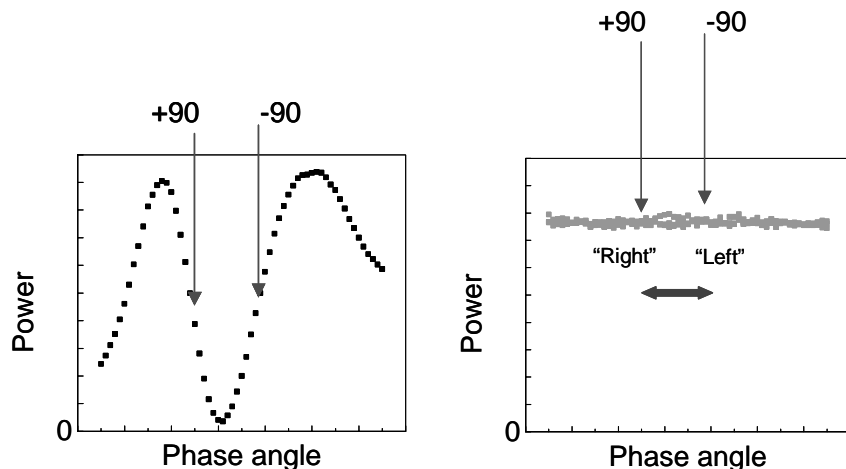


Fig. 7 Left: Inserting a 45° polarizer in the output of the interferometer (not shown in Fig. 6) causes the two orthogonal beams to interfere and the +/- 90° phase shift points set. Right: Linear or circular dichroism is tuned out and the detected signal is independent of phase shift. Modulating back and forth produces a TCD signal if we insert chiral material in the beam.

The TCD is measured by modulating the circular polarization between left and right with the interferometer shown in Fig. 6. In essence, radiation is linearly polarized at 45° to the horizontal and passed through a beam splitter that delivers near equal amounts of vertical and horizontal polarization to the two arms. One arm selects and sends to the detector vertical polarization while the other selects and sends horizontal polarization. By simply changing the path length or “phase” the radiation sent to

the detector can be made to be right or left circularly polarized (or linear if we wish). The material under test is inserted in the beam and the difference between left and right handed polarized transmission measured, as is the total transmission.

The correct path difference or phase shift is easily determined by inserting one more 45° polarizer before the detector (Not shown in Fig. 6). This allows the two otherwise orthogonal polarizations to interfere and the correct setting for right and left determined. As an aside, we note that when properly aligned and tuned, and in the absence of linear or circular dichroism in the path following, the interferometer the detected radiation should be “perfectly” independent of the path difference or phase shift. In practice this “perfection” is achieved by small adjustments of the polarizer in front of the stationary mirror and the position or phase of this reflector.

3. TERAHERTZ CIRCULAR DICHORISM: LYSOZYME

Concentrated solutions of lysozyme in water were contained between two 25μm thick mylar windows stretched over a frame. The TCD signal versus the quantity of lysozyme in the beam was measure at three different frequencies. Fig. 8 displays $\Delta T/T$ normalized by the weight of lysozyme per unit area. To compare with the relative strengths shown in Fig. 3, we recognize that

$$(\alpha_R - \alpha_L) / \alpha \sim -\Delta T / (T \ln(T))$$

and estimate the ratio of difference in extinction coefficients to extinction coefficient to be of the order of 10^{-3} , roughly an order of magnitude larger than shown in Fig. 3, the “mass and spring” model. Three data points do not make a spectrum; a “real” spectrum needs to be recovered; there is an indication of sign change.

The relatively large error bars are largely systematic at this time and not limited by signal to noise ratio in the detector system. The free-electron lasers do exhibit pulse-to-pulse variability in amplitude and frequency. The amplitude fluctuations are partially removed by the reference detector. Pulse to pulse terahertz frequency fluctuations can potentially upset the interferometer. The effect of both amplitude and frequency fluctuations should be minimized but it is clear that a CW source modulated at a convenient detection frequency and a rapid modulation of the polarization should substantially improve the detectable TCD or the noise equivalent TCD.

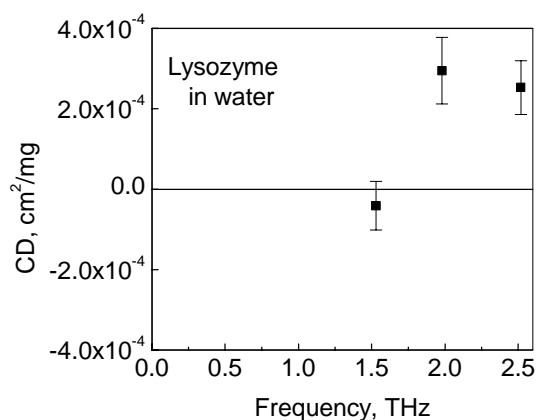


Fig. 8 Terahertz circular dichroism at 1.53, 1.98 and 2.52 THz, $\Delta T/T$ per $\text{mg}\cdot\text{cm}^{-2}$.

4. CONCLUSIONS AND DIRECTION

We have developed simple theoretical models of terahertz circular dichroism in biomolecules and anticipate that with enough sensitivity it is a bio-specific spectroscopy of the macromolecular dynamics of biopolymers. As it should be free of background spectra associated with abiological materials, it is a potentially useful probe of the functionally relevant global biomolecular dynamics as well as a background free method of “finger printing” biological agents.

We have developed a terahertz circular dichroism spectrometer based on a polarization sensitive interferometer and measured for the first time terahertz circular dichroism in a biomolecule, lysozyme. Measurements are made with the biomaterial in water solution; the utility of this approach to biochemical sensing requires being able to carry out spectroscopy in water.

A stable tunable terahertz source at the milliwatt power level would substantially improve this spectroscopy by eliminating residual noise introduced by pulse-to-pulse amplitude and frequency fluctuations from the free-electron lasers. In the absence of this source, we will optimize this instrument and recover representative terahertz circular dichroism spectra to guide further experimental and theoretical work in this potentially rich part of the spectrum.

Acknowledgements:

Funding for the UCSB portions of this research program were provided by NASA (NAG5-12150) and the ARC (DAAD19-02-01-0080), and for the UConn group from the NIH (GM-34548) and NSF (EIA-0129731).

REFERENCES

1. Stryer, L. In: *Biochemistry*, 4th edition. W.H. Freeman and Company, New York pp 150-152 (1995)
2. Zaccai, G., "Moist and soft, dry and stiff: a review of neutron experiments on hydration-dynamics-activity relations in the purple membrane of *Halobacterium salinarum*." *B iophys. Chem.*, **86**, 249-257 (2000)
3. Jeng, M.F., Campbell, A.P. Begley, T., Holmgren, A., Case, D.A., Wright, P.E. and Dyson, H.J. "High resolution solution structures of oxidized and reduced escherichia-Coli thioredoxin." *Structure*, **2**, 853-868 (1994); Kitahara, R., Sareth, S. and Yamada, H. "High pressure NMR reveals active-site hinge motion of folate-bound *Escherichia coli* dihydrofolate reductase." *Biochemistry*, **39**, 12789-12795 (2000)
4. Buck, M. and Karplus, M. "Internal and overall peptide group motion in proteins: molecular dynamics simulations for lysozyme compared with results from X-ray and NMR spectroscopy." *J. Am. Chem. Soc.*, **121**, 9645-9658 (1999); Hinsen, K. "Analysis of domain motions by approximate normal mode calculations." *Proteins*, **33**, 417-429 (1998); Hery, S., Genest, D. and Smith, J.C. "X-ray diffuse scattering and rigid-body motion in crystalline lysozyme probed by molecular dynamics simulation." *J. Mol. Biol.*, **279**, 303-319 (1998); Hinsen, K., Petrescu, A.J., Dellerue, S., Bellissent-Funel, M.C. and Kneller, G.R. "Harmonicity in slow protein dynamics." *Chem. Phys.*, **261**, 25-37, (2000)
5. de Groot, B.L., Hayward, S., van Aalten, D.M.F., Amadei, A. and Berendsen, H.J.C. "Domain motions in bacteriophage T4 lysozyme: A comparison between molecular dynamics and crystallographic data." *Prot. Struct. Func. Gen.*, **31**, 116-127 (1998)
6. Chen, Y.A. and Prohofsky, E.W. "Sequence and temperature-dependence of the interbase hydrogen bond breathing modes in B-DNA polymers, comparison with low-frequency Raman peaks and their role in helix melting." *Biopolymers*, **35**, 573-582 (1995)
7. van Vlijmen, H.W.T. and Karplus, M. "Analysis of calculated normal modes of a set of native and partially unfolded proteins." *J. Phys. Chem. B*, **103**, 3009-3021 (1999); Roitberg, A., Gerber, R.B., Elber, R. and Ratner, M.A. "Anharmonic Wave functions of Proteins: Quantum Self-consistent Field Calculations of BPTI." *Science*, **268**, 1319 (1995)
8. Tama, F., Gadea, F.X., Marques, O. and Sanejouand, Y.H. "Building-block approach for determining low-frequency normal modes of macromolecules." *Prot. Func. Struct. Gen.*, **41**, 1-7 (2000); Brooks, B. and M. Karplus, "Normal modes for specific motions of macromolecules: Application to the hinge bending mode of lysozyme." *Proc. Natl. Acad. Sci. USA*, **82**, 4995 (1985)
9. Kneller, G.R. "Inelastic neutron scattering from damped collective vibrations of macromolecules." *Chem. Phys.*, **261**, 1-24 (2000); Brunori, M. "Structural dynamics of myoglobin." *Biophys. J.*, **86**, 221-230 (2000); Seno, Y. and N. Go. "Deoxymyoglobin Studied by the Conformational Normal Mode Analysis." *J. Mol. Biol.*, **216**, 111-126 (1990)
10. Markelz, A.G., Roitberg, A., and Heilweil, E.J. "Pulsed terahertz spectroscopy of DNA, bovine serum albumin and collagen between 0.1 and 2.0 THz", *Chem. Phys. Lett.* **320**, (2000).
11. Globus, T.R., Woolard, D.L., Samuels, A.C., Gelmont, B.L., Hesler, J., Crowe, T.W., and Bykhovskaia M., (2002) "Submillimeter-wave Fourier transform spectroscopy of biological macromolecules" *J. Appl. Phys.*, **91**, 6105 (2002).
12. Woolard, D.L., Globus, T.R., Gelmont, B.L., Bykhovskaia, M., Samuels, A.C., Cookmeyer, D., Hesler, J.L., Crowe, T.W., Jensen, J.O., Jensen, J.L., and Loerop, W.R. (2002) "Submillimeter-wave phonon modes in DNA macromolecules", *Phys. Rev. E* **65**, 051903/1-11 (2002).
13. Deutsche, C.W. and Moscovitz, A.J., "Optical Activity of Vibrational Origin. I. A Model Helical Polymer", *J. Chem. Phys.*, **49**, 3257 (1968).
14. Deutsche, C.W. and Moscovitz, A., "Optical Activity of Vibrational Origin. II Consequences of Polymer Conformation", *J. Chem. Phys.*, **53**, 2630 (1970).
15. Holzwarth, G. and Chabay, I., "Optical Activity of Vibrational Transitions: A Coupled Oscillator Model", *J. Chem. Phys.*, **57**, 1632 (1972).
16. Schellman, J.A., "Vibrational optical activity", *J. Chem. Phys.* **58**, 2882, (1973).

- 17 Tama, F., Gadea, F.X., Marques, O. and Sanejouand, Y.H. "Building-block approach for determining low-frequency normal modes of macromolecules", *Proteins: Struct. Func. Gen.*, **41**, 1 (2000).
- 18 Fowles G.R. Introduction to modern optics, 2nd Ed., Dover Publications, Inc., New York, (1989).
- 19 Brooks, B. R., Janezic, D. and Karplus, M., "Harmonic analysis of large systems. I. Methodology", *J. Comput. Chem.*, **16**, 1522 (1995).
- 20 Crowe TW, Weikle RM, Hesler JL."GaAs devices and circuits for terahertz applications", International Microwave Symposium Digest (Cat. No.99CH36282). IEEE., **3**, 929 (1999).